Desalination and Water Treatment
www.deswater.com

doi:10.5004/dwt.2018.22472

116 (2018) 195–204
June

Fenton's reagent augmented with TiO_2 for photocatalytic degradation of pulp and paper mill wastewater by plug flow baffle reactor under visible and sunlight irradiation

Ginni Gopalakrishnan, Adishkumar Somanathan*, Rajesh Banu Jeyakumar

Department of Civil Engineering, Regional centre of Anna University, Tirunelveli, Tamilnadu, India,
Tel. + 91 9942491180, email: ginnimuthuvel@gmail.com (G. Gopalakrishnan), Tel. + 91 9841339016, Fax 0462 2552877,
email: adishk2002@yahoo.co.in (A. Somanathan), Tel. + 91 9444215544, email: rajeshces@gmail.com (R.B. Jeyakumar)

Received 11 October 2017; Accepted 6 May 2018

ABSTRACT

The efficiency of solar photocatalytic plug flow baffle reactor by using Fenton's reagent augmented with TiO_2 (solar/Fe^{2+}/TiO_2/H_2O_2) process for the degradation and decolourisation of pulp and paper wastewater has been studied. For this study, a reactor has been designed with pyrexglass in the form of a pond divided with baffle plates. The experiment was performed by varying three significant independent variables such as flow rate in the range of 0–300 mL/min, liquid depth in the range of 2–6 cm and residence time in the range of 0–120 min. The standard response surface methodology (RSM) and central composite design were followed. The maximum COD and colour removal of 98% and 97% respectively was obtained at optimum conditions of flow rate = 75 mL/min, liquid depth = 5 cm and residence time = 75 min. Also, the effect of aeration and without aeration, addition of iron dosage and the kinetics was studied. It was observed that the sequential addition of iron is efficient than single addition and the kinetics followed the pseudo first order reaction with high correlation coefficients. The reaction rate constant for aeration was 2.33 times greater than the reaction without aeration.

Keywords: Plug flow baffle reactor; Pulp and paper mill wastewater; Recirculation flow rate; Liquid depth; Aeration; Treatment cost

---

1. Introduction

The pollutants released from industrial wastewater are under extensive research due to the presence of various organic as well as inorganic pollutants which are further released to the aquatic and soil environment causing human health and ecological problems. Industrial wastewater contains toxic, heavy metals and other organic compounds which are difficult to remove due to their high solubility in water. Treatment of pulp and paper industrial wastewater has been of the intense research because of the enormous water consumption and discharge of pollutants along with the effluents [1]. The wastewater from pulp and paper mill contains high concentrations of ligno-cellulosic materials, phenols, sulphur compounds, high chemical oxygen demand and colour with the presence of suspended, colloidal and dissolved solids. The polymerization between lignin-degraded products and tannin takes place during various pulping and bleaching operations resulting in the formation of complex compounds imparts brown colour [2]. Such colour is not only aesthetically undesirable but also inhibits the natural process of photosynthesis in the wastewater affecting the aquatic eco-system [3]. Chlorinated phenols, guaiacols, catechols, furans, dioxins, aliphatic hydrocarbons, etc., are of prime concern. Some members of this family are known to be toxic, mutagenic, persistent, and bio-accumulating [4].

---

*Corresponding author.

1944-3994 / 1944-3986

Wastewater treatment technologies like gravitational separation, centrifugation, coagulation, adsorption, filtration and other biological methods are largely used [5]. The main treatment processes used at pulp and paper mill plants are primary clarification (sedimentation or floatation), secondary treatment (activated sludge process or anaerobic digestion) and/or tertiary processes [6]. Generally, biological treatment of pulp and paper mill wastewater does not destroy the complex organics. Considerable amounts of recalcitrant organics remain even after treatment and contribute colour and significant amount of the chemical oxygen demand. As a result, the potential for water recycling is significantly reduced by the presence of these recalcitrant organic compounds. The generated wastewater from pulp and paper industry consists of certain organics such as wood extractives, lignin, resins, tannins, synthetic dyes and their degradation products if discharged without proper treatment, the pulp and paper mill wastewater becomes severe threat to aquatic environment [7–9]. In order to improve the discharge quality of wastewater and make the treated wastewater for reuse, an advanced treatment is required.

Advanced oxidation processes (AOPs) is considered to be the most promising technology and they are based on the production of highly reactive hydroxyl radicals which are strong oxidizing agents for the degradation of recalcitrant organic compounds. Solar photo-Fenton process has been established as a principal AOP and the catalyst used in this process is the Fenton's reagent. Solar photocatalytic process is also considered widely for the removal of recalcitrant organic compounds using titanium dioxide as the catalyst [10]. In the case of solar photo-Fenton process, the process is efficient only in acidic pH and therefore the drawback of this process is the pH adjustment. In solar photocatalytic process, TiO_2 is the most promising semiconductor due to its high photocatalytic efficiency is used for the treatment of wastewater. But the disadvantage of the catalyst is sensitive for fouling and slow reaction rate. Also the applications of pure TiO_2 have intrinsic limitations because its band gap located near UV range at $\lambda = 410$ nm render it inactive under the visible light. In order to overcome the above drawbacks and to improve the photoactivity and response to the visible range of light of TiO_2, solar photo-Fenton process and solar photocatalytic process are combined. In this process, TiO_2 is combined with the Fenton's reagent results in the enhancement of hydroxyl radicals in the presence of sunlight under the neutral condition. In photocatalysis process, the illumination of TiO_2 with light energy greater than the band gap energy ejects an electron from the valence band (VB) to the conduction band (CB) creating an hole in the valence band Eq. (1).

$$TiO_2 + h\nu \rightarrow TiO_2(e_{cb}^- + h_{vb}^+) \quad (1)$$

The generation of $OH^\bullet$ as shown in Eq. (2) and with reoxidation of Fe^{3+} by H_2O_2, the reduction through CB electron enables the catalytic cycle of Fe^{3+}/Fe^{2+} [11].

$$Fe^{2+} + H_2O_2 \rightarrow Fe^{3+} + OH^\cdot + OH^- \quad (2)$$

The presence of Fe^{3+} species on the photocatalytic activity act as h^+/e^- traps thus hindering the recombination rate and enhancing the photocatalytic rate. Thus the industrial application of a photocatalytic process needs a photo reactor which can efficiently bring solar photons and chemical reagents into contact with the photocatalyst. The photons from the solar irradiation are utilized for the degradation of wastewater in solar photocatalytic reactors.

Therefore, different types of solar photocatalytic reactors have been designed for the degradation of organic compounds and are classified as concentrating and non-concentrating reactor systems based upon absorption of sunlight [12]. Non-concentrating reactors absorb direct and diffuse solar radiation with negligible optical losses whereas in a concentrating reactor system, the sunlight is concentrated thus decreasing the size of the reactor compared to non concentrating reactor [13]. Photocatalytic water treatment reactors such as parabolic trough reactor, thin film fixed bed reactor, compound parabolic collecting reactor, double skin sheet reactor, fluidized bed reactor, pebble bed reactor etc., are commonly used treatment techniques [14]. But the above solar photocatalytic reactors have their own advantages and disadvantages. Singh et al. [15] studied the photocatalytic oxidation of synthetic wastewater containing high COD using a parabolic trough reactor. TiO_2 has been used as a photocatalyst. It was reported that the maximum COD reduction of 86% was obtained. The disadvantages of parabolic reactors are it can receive only direct radiation, high cost due to tracking system and low quantum efficiency with TiO_2. In another literature, [16] developed a solar fixed bed reactor using a very stable and active TiO_2 film supported on a glass plate for the mineralization of dichloroacetic acid. Although the system is efficient in the photodestruction of dichloroacetic acid, large volumes of wastewater needs larger working areas to produce thin films over the illuminated catalyst. Velegraki et al. [17] treated the winery effluents by the solar light-driven Fenton process by a pilot compound parabolic collector (CPC) and obtained the efficient mineralization and detoxification of winery wastewater. In a literature, [18] designed the fluidized bed reactor and calculated the flow rate for the complete fluidization and the settling velocity of the particles. Though the fluidized bed reactor has been used for the wastewater treatment, it has the limitations such as that the reactors require larger vessels with high initial capital cost for industrial application. Dillert et al. [19] treated the various biologically pretreated industrial wastewater in double skin sheet reactor. The drawback of this reactor is that it can be operated in slurry mode and they suffer from low optical efficiency. Rao et al. [20] studied a novel, low cost, pebble bed photocatalytic reactor (PBPR) having a horizontal or inclined solar trough collector contains TiO_2 coated, silica rich, white pebbles fixed on a flat surface in an ordered configuration to facilitate the contact between the liquid and the photocatalyst. The main disadvantage of pebble bed reactor is characterized by a laminar flow and therefore the reactor experiences limited degradation efficiency. Though many studies have been reported on the efficient use of various reactors, the application of reactors at large scale are lacking due to opacity, light scattering and depth of radiation penetration. There are several designs of solar reactors to concentrate and use efficiently the solar irradiation in the solar photo-Fenton process [21]. PFRs are usually preferred due to their simple design and fabrication. The reactor also absorbs the incident light, promoting photocatalytic reactions in an effective manner with minimal photonic losses as the plug flow reactor is a long tank with high length-to-width ratio.

In the present study solar photocatalytic plug flow baffle reactor, a non-concentrating solar photocatalytic reactor has been designed for cost effectiveness, less reaction time and effective degradation and removal of COD and colour for the treatment of pulp and paper mill wastewater using Fenton's reagent augmented with TiO_2 (solar/Fe^{2+}/TiO_2/H_2O_2) process. The aim of this study is to investigate the performance efficiency of the reactor and the influencing parameters such as liquid depth, recirculation flow rate and residence time are studied by optimization using response surface methodology.

2. Materials and methods

2.1. Source and characterization of the wastewater

The wastewater samples used was obtained from the pulp and paper mill located near Erode, Tamil Nadu, India. The raw wastewaters from various unit operations namely pulping, pulp washing, bleaching and paper making process are mixed together and the amount of wastewater discharged from the mill is 15,000 m^3/d. The samples were collected from the collection tank without modifications. The samples were transported to the laboratory in plastic cans and stored at 4ºC. The physicochemical characteristics of the wastewater were analyzed as per standard methods [22] and it was determined as pH = 6.99 ± 0.1, colour (at 465 nm) = 0.848 ± 0.100, COD = 1800 ± 400 mg/L, BOD = 400 ± 50 mg/L and BOD_5/COD = 0.22 ± 0.05.

2.2. Chemical reagents

The experiments were performed using ferrous sulphate heptahydrate ($FeSO_4{\cdot}7H_2O$) reagent-grade hydrogen peroxide (H_2O_2) (30%, w/w, Merck) to obtain hydroxyl radical $OH^{\bullet}$. Sulphuric acid (H_2SO_4) and sodium hydroxide (NaOH) were used for the pH adjustment. The photocatalyst employed was commercial TiO_2 (P-25), supplied by Degussa (Germany). According to the manufacturer's specifications, P-25 has an elementary particle size of 30 nm, Brunauer, Emmett and Teller (BET) specific surface area of 50 m^2/g and crystalline mode comprising 80% anatase and 20% rutile. Sodium thiosulphate ($Na_2S_2O_3$), potassium dichromate ($K_2Cr_2O_7$), mercuric sulphate ($HgSO_4$), and ferrous ammonium sulphate ($Fe(NH_4)_2(SO_4)_2{\cdot}6H_2O$) were used for COD analysis. Sodium sulphite (Na_2SO_3) was used to quench the reaction. All the reagents used in this experiment were of analytical grade and used were received without further purification.

2.3. Solar photocatalytic reactor

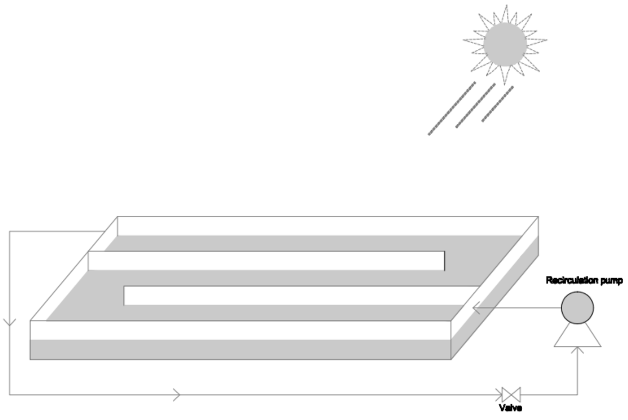

Fig. 1. Solar photocatalytic plug flow baffle reactor.

A non-concentrating solar photocatalytic plug flow baffle reactor was fabricated. It is a suspended type catalytic reactor system having no UV transparent walls and solar tracking system. The schematic diagram of photocatalytic plug flow baffle reactor is shown in Fig. 1. The solar photocatalytic plug flow baffle reactor is made of pyrex glass of size 45 cm × 21 cm x 8 cm in the form of a pond divided with baffle plates at a spacing of 7 cm. The irradiated surface area for the solar photocatalytic plug flow baffle reactor is 0.09 m^2. A recirculating pump was used to recycle the wastewater continuously and uniform mixing of wastewater was done by supplying air using aerators.

2.4. Experimental

All photocatalytic experiments were carried out at Anna University Campus, Tirunelveli, India (8°44´N 77°44´E). The experiments were done in a solar photocatalytic plug flow baffle reactor. Experiments were conducted under solar illumination on clear sky days from January to April with the solar light intensity 103±2 W/m^2. Evaluation of the performance of solar photocatalytic reactor was carried out by Fenton's reagent augmented with TiO_2 (solar/Fe^{2+}/TiO_2/H_2O_2) process. The optimum chemical dosages for the experiments were taken from the results as previously reported [23]. Initially, the optimum amount of TiO_2 and ferrous sulphate was homogenised and then it was transferred to the wastewater and were stirred in the dark to attain the adsorption–desorption equilibrium. Finally, the required amount of hydrogen peroxide (H_2O_2) was added to the wastewater and irradiation was carried out in the open air using a pump for continuous aeration to provide oxygen and completely mix the reaction mixture. The samples were taken from the solar photocatalytic plug flow baffle reactor at specific time intervals for COD and colour analysis. To the collected samples, quenching was done by adding sodium sulphite solution (2 mL) and then samples were filtered through filter paper (0.42 µm Millipore membrane) to remove the catalyst. The COD was determined using the dichromate closed reflux method according to standard method. Biochemical oxygen demand (BOD_5) was determined at 20ºC using the standard dilution technique according to [22]. All the experiments were performed in triplicate.

2.5. Central composite design

Response surface methodology (RSM) is a useful technique for obtaining the optimum conditions of a process for the best response. The design of experiments involves the optimization of response influenced by the independent variables. ANOVA test was used to study the variation of results obtained from the model and determine whether the results are significant with the model. The analysis of regression and statistical analysis were performed by the Design Expert 8.0.7 software. The significance of probability values are verified by P-values if the P-value is less than 0.05. The least value of coefficient of variation (CV = 7.51% for COD and 5.66% for colour) indicates the degree of accuracy and reliability of the experiments. After conducting the preliminary runs, the range of the parameters were fixed. In this study, three independent variables such as flow rate is varied from 0 to 300 mL/min, residence time in the range of 0–120 min, and liquid depth in the range of 2–6 cm were studied. The following Eq. (3) is used to achieve COD and colour removal.

$$Y = b_0 + \Sigma\, b_i X_i + \Sigma\, b_{ii} X_i^2 + \Sigma\, b_{ij} X_i X_j \qquad (3)$$

where Y is the predicted response factor, b_0 is the coefficient of the intercept, b_i is the coefficient of the linear term, b_{ii} is the coefficient of the quadratic term, b_{ij} is the coefficient of interaction, X_i and X_j are the input coded variables that influence the response (Y). The design consisted of 2^k factorial points augmented by 2k axial points and a centre point, where k is the number of variables. A set of 20 experiments (= $2^k + 2k + 6$) were designed to optimize the condition for the COD and colour removal efficiencies of pulp and paper mill wastewater by solar/Fe^{2+}/TiO_2/H_2O_2.

3. Results and discussions

3.1. Design matrix fitting and statistical analysis

The following regression Eqs. (4) and (5) show the degradation efficiencies of COD and colour removals.

$$\text{COD (\%)} = +\,65.78 - 10.06\,A + 16.31\,B - 5.75\,C - 11.12\,AB + 3.38\,BC \qquad (4)$$

$$\text{Colour (\%)} = +\,69.34 - 12.50\,A + 14.75\,B - 4.25\,C + 12.25\,AB + 2.75\,BC \qquad (5)$$

In Eqs. (4) and (5), the independent variables A, B, C, the interaction variables AB, BC are significant model terms with the probability value less than 0.05. The other model terms are insignificant and were removed from the equation. The lack of fit values for COD and colour removal were 0.2835 and 0.2229 respectively thus implies insignificant with the fitted model and the response surfaces were sufficiently explained by the regression equation. The degradation efficiency increases with the increasing residence time as can be inferred by the positive linear coefficient. However an inhibitory effect is observed with the values of flow rate and liquid depth according to the negative coefficient. Similarly for colour removal, the test variables such as A, B, C, AB, BC are significant and the remaining insignificant model terms are eliminated. Analysis of variance was used to analyze the experimental data for both COD and colour removal and the results are shown in Table 1. Data given in the table demonstrates that the F-values for the models are 52.36 and 87.94 are significant for the responses COD and colour respectively. P-values are used to check the significance of each coefficient and the corresponding p-values are <0.0001 and there is only a 0.01% chance of occurrence of model F-value because of noise.

The predicted R^2 value of 0.9792 and 0.9875 for COD and colour removal explains the goodness of fit and is in agreement with the adjusted R^2 values. Adequate precision measures the signal to noise ratio. A ratio greater than 4 is desirable. In this study, the ratio of 26.726 indicates an adequate signal for COD removal and 33.575 for colour removal.

3.2. Effect of recirculation flow rate

To determine the effect of recirculation flow rate, the recycle flow rates are varied between 0 and 300 mL/min. Figs. 2a and 2b represent the 3D response surface plots as a function of two variables maintaining all others at the fixed levels. From the figure, it is clear that the flow rate and residence time are the influential parameters on COD and colour removal. According to the shape of the 3D surface; larger amplitudes of COD and colour removal are obtained by varying the flow rate and residence time, it can be concluded that the flow rate is more influential parameter than residence time.

The degradation profile for different flow rates and their kinetics are given in Fig. 3. It is clear that when there is no flow rate, the COD and colour removal efficiency is very low. Regarding the kinetics, the rate constant for the process without recycle flow rate is 0.0092 min^{-1}. These can be explained as when there is no flow rate, the reaction takes place in two theoretical zones such as an illuminated zone and a dark zone. The catalyst absorbs the radiation in the illuminated region whereas the radiation cannot penetrate in the dark region causing the reduction in the removal efficiency. As the flow rate increases, the degradation efficiency also increases. Thus when the flow rate is at 75 mL/min, the maximum COD and colour removal efficiency is obtained. When the flow rate is increased above 75 mL/min, there is a decrease in COD and colour removal. This is because at flow rate of 75 mL/min, the degradation efficiency is increased with the increase in hydraulic retention time of wastewater leading to an increase in an active radical species production and improves the photocatalytic reaction between contaminant and catalyst by increasing diffusion. But when the flow rate is increased above 75 mL/min, the hydraulic retention time of wastewater is decreased and the contact time is increased to achieve the maximum COD and colour removal because of the limitation of sunlight penetrating into the reactor with the rise in liquid film thickness [24]. Also the number of times the wastewater enters the reactor increases thereby decreasing the efficiency [20]. Thus the increase in flow rate from 150 mL/min to 300 mL/min led to the decrease in COD from 85% to 40%. Regarding the kinetics, it is found that the kinetic rate constant for the reaction at a flow rate of 75 mL/min is 0.0546 min^{-1}. The kinetic rate constants for the flow rates of 150 mL/min, 225 mL/min and 300 mL/min were 0.0267 min^{-1}, 0.0184 min^{-1} and 0.0099 min^{-1} respectively. It was observed that the rate of the reaction increases

Table 1
ANOVA results of the response surface quadratic model for COD and colour removal

	Source	Sum of squares	df	Mean squares	F value	p-value Prob > F
COD	Model	8560.58	9	951.176	52.3621	< 0.0001
	Residual	181.653	10	18.1653		
	Lack of fit	114.82	5	22.964	1.71801	0.2835
	Pure error	66.8333	5	13.3667		
	Cor total	8742.24	19			
Colour	Model	9089.71	9	1009.97	87.9449	< 0.0001
	Residual	114.841	10	11.4841		
	Lack of fit	77.3409	5	15.4682	2.06242	0.2229
	Pure error	37.5	5	7.5		
	Cor total	9204.55	19			

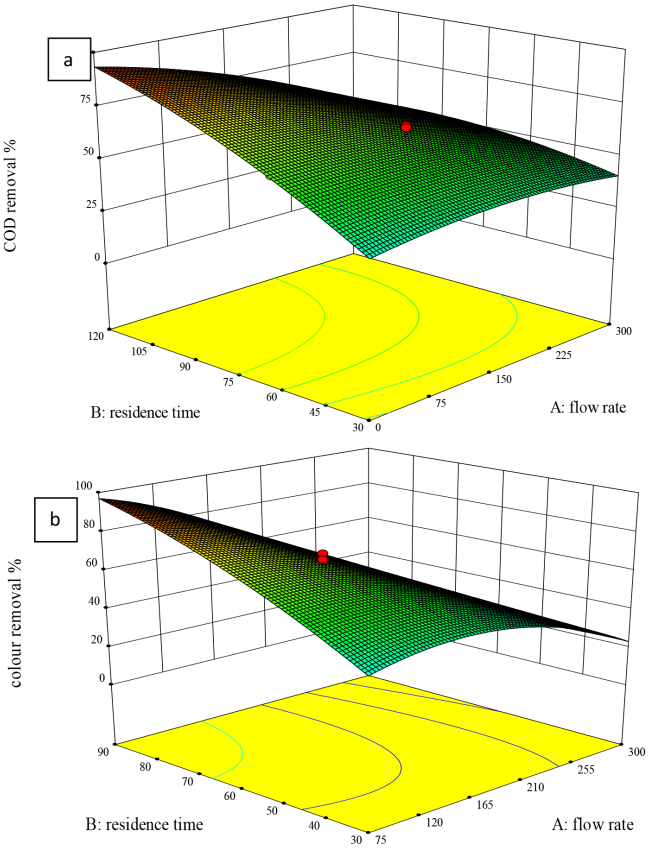

Fig. 2. (a) and (b) 3D surface plots showing the effects of mutual interactions between residence time and flow rate on COD and colour removal efficiency (pH = 7, Fe^{2+} = 0.10 g/L, TiO_2 = 0.13 g/L, H_2O_2 = 1.80 mL/L, solar light intensity = 103±2 W/m^2).

with the flow rate from 0 mL/min to 75 mL/min and then decreases when the flow rate is further increased above 75 mL/min. Thus it was observed reaction rate for the flow rate 75 mL/min is 5.93 times faster than the rate of the reaction without recycle flow rate. Thus the optimum flow rate was taken as 75 mL/min. Similar result was reported in a literature in which the photocatalytic activity of N-ZnO @ PF for the degradation of amaranth were determined at flow rates of 80 mL/min, 100 mL/min and 120 mL/min and obtained the greatest efficiency at a flow rate of 80 mL/min [25]. In another literature, the degradation efficiency of phenol was studied with two different flow rates 1.2 L/min and 1.6 L/min and it was found that the lower flow rate is better compared to higher flow rate [26].

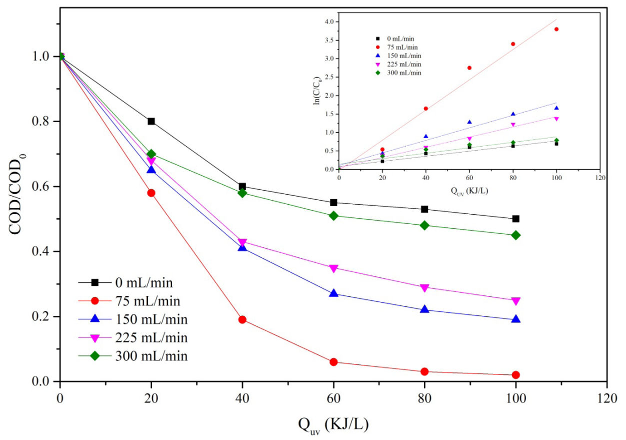

Fig. 3. Degradation profile for different flow rates and the inset panel shows its kinetic analysis assuming that COD follows the pseudo-first-order reaction.

3.3. Effect of liquid depth

To find the effect of liquid depth, the volume of wastewater samples from 2 L to 6 L were taken with the corresponding depths varying from 2 cm to 6 cm which is shown in Figs. 4a and 4b as 3D response surface plots. In the figure, the influence of liquid depth and the residence time on the COD and colour removal of pulp and paper mill wastewater is presented. According to the shape of the 3D surface; larger amplitudes of COD and colour removal are obtained by varying the liquid depth and residence time, it can be concluded that the liquid depth is more influential parameter than residence time. It was observed from the figure that when the liquid depth is increased, the residence time is also increased. But the COD and colour removal efficiency decreased.

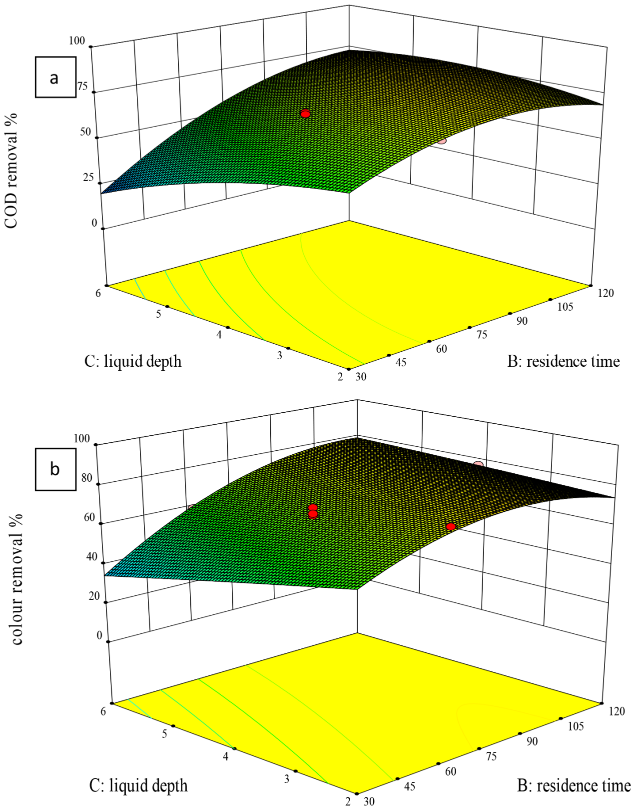

Fig. 4(a) and (b). 3D surface plots showing the effects of mutual interactions between liquid depth and residence time on COD and colour removal efficiency (pH = 7, Fe^{2+} = 0.10 g/L, TiO_2 = 0.13 g/L, H_2O_2 = 1.80 mL/L, solar light intensity = 103±2 W/m^2).

The experimental values of COD removal efficiency were determined by varying the depths from 2 cm to 6 cm with the flow rate of 75 mL/min and the kinetic rate constants for the reaction are also obtained which are shown in Fig. 5. It was clear that the degradation for all liquid depths is faster at 15 min of the reaction since it is independent of irradiation and more number of hydroxyl radicals are generated because of the reaction between Fe^{2+} and hydrogen peroxide given in Eqs. (6) and (7) [27].

$$Fe^{2+} + H_2O_2 \rightarrow Fe^{3+} + OH^- + HO^\bullet \tag{6}$$

$$Fe^{3+} + H_2O + h\nu \rightarrow Fe^{2+} + HO^\bullet + H^+ \tag{7}$$

After this, the COD removal efficiency is decreased as the liquid depths increased. The reaction rate constants for the liquid depths 2 cm, 3 cm, 4 cm, 5 cm and 6 cm were 0.0717, 0.0649, 0.0601, 0.0546 and 0.0184 respectively. Thus the reaction rate decreases with the increase in liquid depth. Regarding the COD removal, when the depth is 2 cm, the maximum removal of COD was obtained at 45 min of treatment. For the depth of 5 cm, the maximum removal percentage of COD is obtained at 75 min of treatment. Thus the increase in the liquid depth decreases the COD removal efficiency with the increase in the reaction time of the wastewater in the reactor. When the depth is increased above 5 cm, there is a drastic decrease in degradation. This is because for the same surface area, the photons entering the reactor are also the same. But due to the increase in liquid depth, the solar light cannot penetrate to the bottom of the reactor and the absorption of UV light blocks the photons from reaching the active reaction sites. Also the increase in liquid depth increases the volume of wastewater due to which the Fe concentration increases which give rise to more iron ions and it needs to be photoactivated. This results in the decreased removal efficiency. Thus from the figure, it was observed that with the increase in liquid depth from 2 cm–6 cm, the COD removal efficiency decreased from 99% to 60%. In a literature, the author studied the degradation of micropollutants by solar photo-Fenton process with the liquid depth of 5 cm and 10 cm. It was reported that the liquid depth 10 cm is recommended since more volume could be treated with the high process rate per surface unit [27].

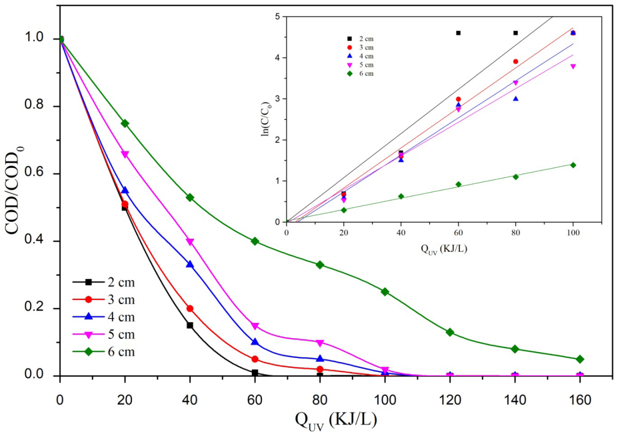

Fig. 5. Degradation profile for liquid depth and the inset panel shows its kinetic analysis assuming that COD follows the pseudo-first-order reaction.

3.4. Effect of aeration in reactor

To find the effects of aeration on the performance of the solar photocatalytic plug flow baffle reactor, the experiment was conducted with aeration and without aeration for the optimum conditions. The results are shown in Fig. 6. It was clear that the COD and colour removal of 98% and 97% respectively was obtained at 45 min of treatment with aeration at an air flow rate of 3.2 L/min whereas 87% and 85% of COD and colour removal respectively was obtained at 45 min of treatment without aeration. This is because the presence of oxygen is beneficial and to avoid recombination, an electron acceptor must be present. The electron acceptor oxygen is used for transferring an electron in the reaction with the photocatalyst. Hydrogen peroxide or peroxide anion are produced by the dismutation of superoxide anion or its protonated form. It also provided more active sites for photogenerated electrons which subsequently interact with oxygen or to react with other electron acceptors given in Eq. (8) to Eq. (16). These reactions are oxygen generating or oxygen consuming by the reaction of the radicals with organic matter, hydrogen peroxide or with other radicals.

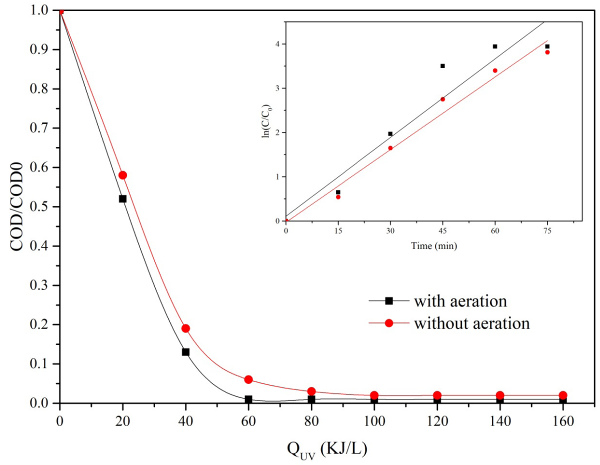

Fig. 6. Effect of COD removal with and without aeration and the inset panel shows its kinetic analysis assuming that COD follows the pseudo-first-order reaction.

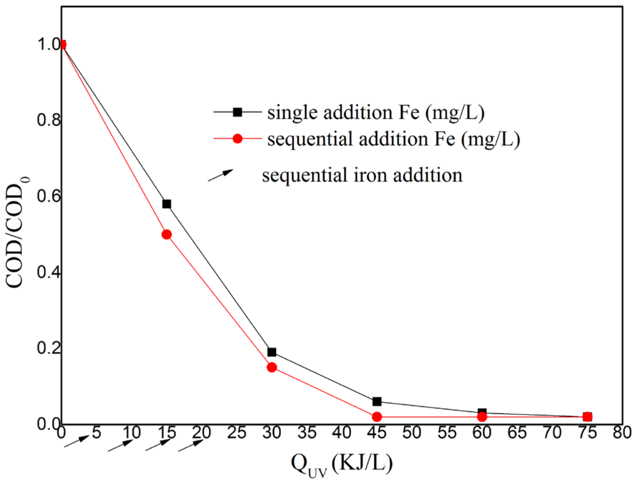

Fig. 7. Effect of COD removal on single and sequential addition of iron.

$$Fe^{3+} + e^- \rightarrow Fe^{2+} \tag{8}$$

$$Fe^{2+} + O_{2(ads)} \rightarrow Fe^{3+} + O_2^{\bullet -} \tag{9}$$

$$TiO_2 + O_2 \rightarrow O_2^{\bullet -} \tag{10}$$

$$O_2^{\bullet -} + 2\,H^+ \rightarrow H_2O_2 \tag{11}$$

$$H_2O_2 + TiO_2 \rightarrow HO^\bullet + HO^\bullet \tag{12}$$

$$O_2^{\bullet -} + H_2O_2 \rightarrow HO^\bullet + HO^\bullet + O_2 \tag{13}$$

$$O_2^{\bullet -} + H^+ \rightarrow HO_2^\bullet \tag{14}$$

$$2\,HO_2 \rightarrow H_2O_2 + O_2 \tag{15}$$

$$O_2^{\bullet -} + HO_2^\bullet + H^+ \rightarrow H_2O_2 + O_2 \tag{16}$$

The reaction follows the first order and the reaction constants for the process with aeration are 0.06 min^{-1} and for without aeration are 0.045 min^{-1}. Similar results were obtained for the degradation of p-Np at an optimum air flow rate of 0.4 L/min [28]. Shavisi et al. [29] studied the effect of aeration for the degradation of ammonia at a flow rate of 10 L//min and obtained the removal efficiency of 75%.

3.5. Effect of iron dosage strategy

To study the effect of iron dosage strategy, the iron was added sequentially and pulse (single addition) conditions. The two conditions were compared and it was found that when the iron is added sequentially for every 5 min at a dosage of 25 mg/L, the degradation efficiency is greater than the pulse addition(100 mg/L Fe^{2+}). The results are given in Fig. 7. From the graph, it was observed that about 98% of COD removal is obtained at 45 min of treatment for sequential addition. But the same removal percentage is obtained at 75 min of treatment when added in pulse condition. The difference between the two strategies is when the iron was added in large amount, the iron precipitation is more than when it was added sequentially. When the first iron addition was completed, the ferrous iron oxidation takes place yielding hydroxyl radicals causing a reduction in iron. In addition to that iron hydrolysis drop pH thereby dissolving the iron and the reaction takes place given in Eq. (17).

$$Fe^{3+} + H_2O \rightarrow Fe(OH)_3 + H^+ \tag{17}$$

The second and third addition causes a quick generation of new hydroxyl radicals and the degradation of wastewater continues. Therefore the sequential addition of iron is more efficient than the single addition.

3.6. Fe^{2+} profile and H_2O_2 consumption

The maximum COD and colour removal, Fe^{2+} profile, H_2O_2 consumption and pH profile are shown in Fig. 8. There is a fast decrease in COD and colour removal due to more oxidized organic intermediates formed at the beginning of the process and afterwards, the COD and colour gradually decreases. This behavior may be explained because the H_2O_2 has been consumed rapidly at the beginning and then gradually decreases thus no more $OH^\bullet$ radicals are formed [30]. Regarding iron profiles, there was a faster iron reduction and the Fe^{2+} oxidation was instantaneous. After that, the iron concentration remained constant throughout the experiment but decreased by the end due to the formation of complex products with low-molecular-weight carboxylic acids [31].

3.7. Electrical energy per order (EEO)

The right approach to optimize the performance is crucial in order to minimize the operation cost for industrial wastewater treatment processes. Hence, a figure-of-merit, electrical energy per order (EEO) was used to assess the cost

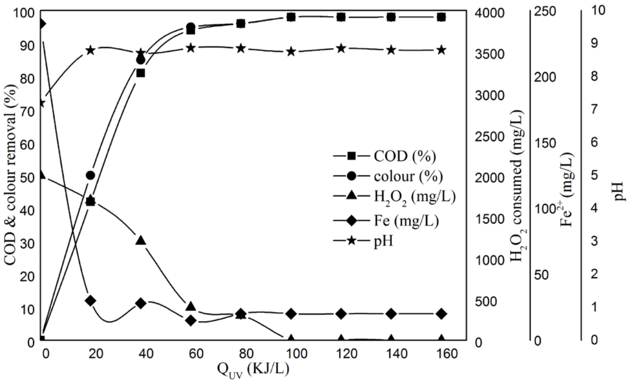

Fig. 8 Effect of COD, colour removal, Fe^{2+} concentration, H_2O_2 consumption and pH removal under optimum conditions.

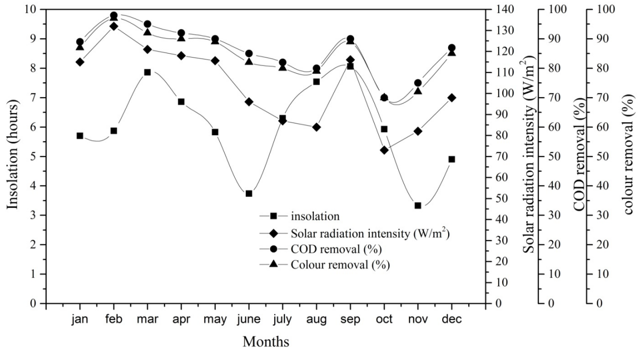

Fig. 9. Average global radiation, insolation with the COD and colour removal during the year 2015.

efficiency of the optimum degradation process [32]. According to Photochemistry Commission of International Union of Pure and Applied Chemistry, the EEO was defined as the KWh of electrical energy needed to decrease the concentration of a contaminant by one order of magnitude in 1 m^3 of contaminated water [33]. It can be calculated using Eq. (18)

$$EEO = \frac{P \times t \times 1000}{V \times 60 \times \log\left(\frac{Ci}{Cf}\right)} \tag{18}$$

where P is the related power (KW) of the AOP system, t is the irradiation time (min), V is the volume of the water in the reactor (L), C_i and C_f are the initial and final concentration of the pollutant. The electrical energy required per m^3 is 15.12 kWh. The cost of electricity is 0.13 U$ per KWh, the contribution to the treatment cost from electrical energy will be 1.9656 U$.

3.8. Economic evaluation of the solar/Fe^{2+}/TiO_2/H_2O_2 process in a solar photocatalytic plug flow baffle reactor

In spite of the degradation efficiency of solar/Fe^{2+}/TiO_2/H_2O_2 process for the removal of organic pollutants in pulp and paper mill wastewater, the economic analysis must also be evaluated. For economic analysis, new technologies are considered for reducing the processing costs over other technologies [34]. The economic evaluation is based on the treatment of pulp and paper mill wastewater of capacity 15,000 m^3/d. The cost analysis mainly comes from the reagent consumption. The chemical costs include consumables such as the catalysts Fe^{2+}, TiO_2 and H_2O_2. The pilot plant reactor was designed to treat the pulp and paper mill wastewater for 98% COD and 97% colour removal. For each day, the average useful hours were found to be 6 h. The Fig. 9 shows the average global radiation, total insolation, COD and colour removal during the various months of the year. The yearly average solar light intensity for the experimental study was estimated at 103 ± 2W/m^2.

The area of the pilot scale reactor was found to be 13,994 m^2. In order to apply the treatment process studied in the present work on an industrial scale, the total installed cost and the operating costs for the treatment of pulp and paper mill wastewater was evaluated. The facility cost, contingencies, engineering and spare parts altogether comes under the total installed costs. The personnel and materials costs necessary to operate and maintain the facility, chemical provisions and electrical energy costs comes under the operational costs [34]. The total yearly cost for the treatment of pulp and paper mill wastewater is based on the initial installation cost and the operating costs. The reusability and recyclability of the catalyst was considered and it was observed that the removal efficiency was above 90% for the first five consecutive trials. Hence the catalyst could be recycled for atleast five trials. In cost analysis, the recycle of the catalysts were also considered.

The overall costs for the treatment of pulp and paper mill wastewater by solar/Fe^{2+}/TiO_2/H_2O_2 process were calculated to achieve COD value of 250 mg/L which can be discharged and used as irrigation water and to a value of 40 mg/L to achieve maximum removal efficiency of 98%. The treated characteristics of the pulp and paper mill wastewater are given in Table 2. The estimated annual treatment cost is given in Table 3. The yearly capital cost and operational cost are given in Fig. 10. This amount can be amortized along 20 years with a 12% FCR. Regarding the optimum conditions to achieve a COD target of 250 mg/L, the annual treatment cost of 1.39U$ and for 40 mg/L, the annual treatment cost of 14 U$ were obtained. The Fig. 11 shows the operational costs per gram of COD removed. The main cost for this process is initially reagents, which account for more than 97% of the total costs. In this study, as the wastewater was treated at neutral pH, there was no need to adjust the pH for acidifying the wastewater thereby reducing consumption cost of sulphuric acid. Also the advantage of solar/Fe^{2+}/TiO_2/H_2O_2 process is that shorter reaction time and lower reagent consumption with the consequent reduction in operating cost. Torres-Socias et al. [35] studied the economic assessment of landfill leachate by solar photo-Fenton process with the design flow rate of 40 m^3/d and the estimated treatment cost was 43 €/m^3 (45.15 U$). In a literature, the total cost of solar photo-Fenton process and for a five year operation, for the treatment capacity of 50 m^3/d is estimated to be approximately 2.11 €/m^3 (2.2155 U$) [36]. Selvabharathi et al. [37] carried out a cost analysis by analyzing the degradation of tannery wastewater by the combined homogeneous and heterogeneous process and estimated the annual treatment cost as 19.35 U$. Thus the above literature discussed the cost of treatment for vari-

Table 2
Characteristics of treated pulp and paper mill wastewater

Parameters	Solar/Fe^{2+}/TiO_2/H_2O_2	Minimal National Standards (MINAS) for disposal
pH	7	6.5–9.0
TSS (mg/L)	30	100
COD (mg/L)	40	250
BOD_5 (mg/L)	30	30
BOD_5/COD	0.75	–

Table 3
Estimated annual treatment cost(US$)

Process			Solar/Fe^{2+}/TiO_2/H_2O_2
A	Facility cost		1122786
B	Project contingency	15% of A	168418
C	Engineering and set up	50% (A+B)	645602
D	Spare parts	0.5% (A+B)	6456
E	Total installed cost	A+B+C+D	1943262
F	Personnel cost	0.25 man year	4022
G	Maintenance material cost	2% (A+B)	25824
H	Electricity	5 kW/h (1752 h)	39420
I	Chemical		74214468
J	Total operating cost	F+G+H+I	72794835
K	Annual levelized cost	E × FCR + J	73121692
L	Annual treatment cost	K/(15000 × 365)	14

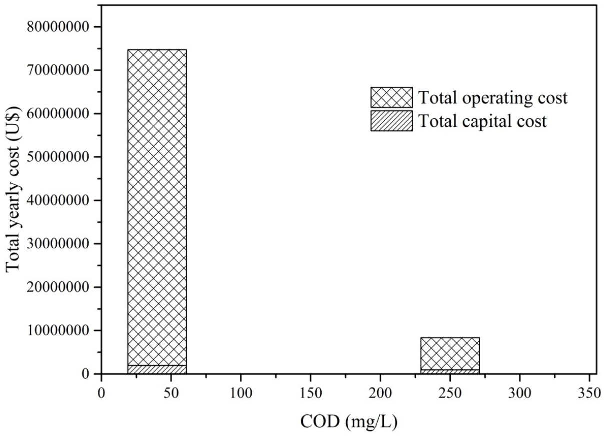

Fig. 10 Total yearly capital and operation costs for the optimum conditions.

ous advanced oxidation processes. It was observed that treatment cost of the individual process is more compared to the combined process. In this study, the cost is mainly reduced by using the natural resource sunlight for the solar/Fe^{2+}/TiO_2/H_2O_2 process providing an economic feasibility on industrialization as long as to overcome technical challenges. The solar/Fe^{2+}/TiO_2/H_2O_2 process is economically more efficient when the target COD is 250 mg/L and below. Though the above literature studied the treatment cost of two different advanced oxidation processes, the estimated treatment cost is 3.2 times greater than the process of this study.

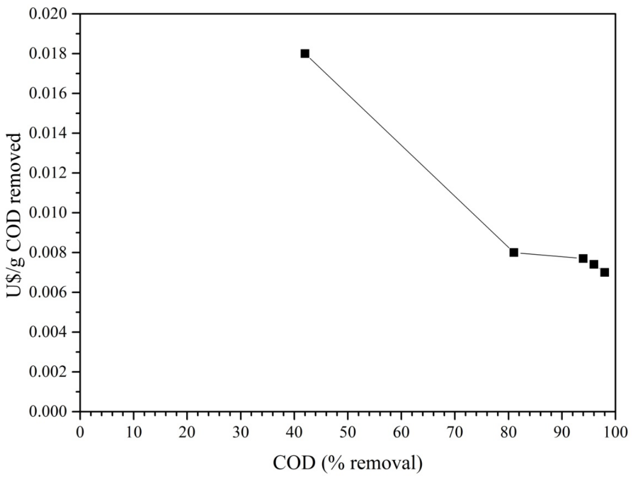

Fig. 11. Total operational cost for the optimum conditions per gram of COD removed.

4. Conclusion

The solar photocatalytic plug flow baffle reactor for the treatment of pulp and paper mill wastewater was successfully designed using solar light. The effect of significant operational parameters such as recirculation flow rate, liquid depth, residence time, with aeration and without aeration, addition of iron dosage was determined. The results indicate that the degradation efficiency increases as the recirculation flow rate increases and decreases after the optimum value due to the decreased hydraulic retention time. The effect of liquid depth influences the degradation efficiency by the fact that with the increase in liquid depth, the degradation efficiency decreases because the penetration of sunlight cannot reach the bottom of the reactor. The effect of aeration improves the degradation efficiency by the increasing dissolved oxygen which acts as the electron acceptor. The results also indicate that the sequential addition of iron is more efficient than the single addition. Kinetic study reveals that the degradation of pulp and paper mill wastewater fitted first order kinetics. The cost analysis for the treatment using the solar/Fe^{2+}/TiO_2/H_2O_2 process to achieve COD values of 250 mg/L and 40 mg/L are 1.39 U$ and 14 U$ respectively.

References

[1] M.S. Vohra, M.S. Al-Suwaiyan, M.H. Essa, M.M.I. Chowdhury, M.M. Rahman, M.M. Labaran, Application of solar photocatalysis and solar photo-fenton processes for the removal of some critical charged pollutants: mineralization trends and formation of reaction intermediates, Arab J. Sci. Eng., DOI 10.1007/13369-015-2021-2.

[2] T. Kreetachat, M. Damrongsri, V. Punsuwon, P. Vaithanomsat, C. Chiemchaisri, C. Chomsurin, Effects of ozonation process on lignin – derived compounds in pulp and paper mill effluents, J. Hazard. Mater., 142 (2007) 250–257.

[3] V. Saravanan, T.R. Sreekrishnan, Bio-physico-chemical treatment for removal of colour from pulp and paper mill effluents, J. Sci. Ind. Res., 64 (2005) 61–64.

[4] R. Maheshwari, B. Rani, A. Saxena, M. Prasad, U. Singh, Analysis of effluents from recycled paper industry, J. Adv. Sci. Res., 3(1) (2012) 82–85.

[5] G. Boczkaj, A. Fernandes, Wastewater treatment by means of advanced oxidation processes at basic conditions: A review, Chem. Eng. J., 320 (2017) 608–633.

[6] K. Eskelinen, H. Sarkka, T.A. Kurniawan, M.E.T. Sillanpaa, Removal of recalcitrant contaminants from bleaching effluents in pulp and paper mills using ultrasonic irradiation and Fenton-like oxidation, electrochemical treatment, and/or chemical precipitation: A comparative study, Desalination, 255 (2010) 179–187.

[7] N. Kumara Swamy, Paper mill effluent: Decolourisation and detoxification studies using chemical and microbial methods, Jaypee Institute of Information Technology, 2012.

[8] I. Qadir, R.C. Chhipa, Critical evaluation of some available treatment techniques for textile and paper industry effluents: a review, Am. Chem. Sci. J., 6(2) (2015) 77–90.

[9] C.H. Ko, C. Fan, Enhanced chemical oxygen demand removal and flux reduction in pulp and paper wastewater treatment using laccase-polymerized membrane filtration, J. Hazard. Mater., 181 (2010) 763–770.

[10] N.B. Parilti, D. Akten, Optimization of TiO_2/Fe(III)/solar conditions for the removal of organic contaminants in pulp mill effluents, Desalination, 265 (2011) 37–42.

[11] H.E. Kim, J. Lee, H. Lee, C. Lee, Synergistic effects of TiO_2 photocatalysis in combination with Fenton-like reactions on oxidation of organic compounds at circumneutral pH, Appl. Catal. B: Environ., 115–116 (2012) 219–224.

[12] S. Kanmani, K. Thanasekaran, D. Beck, Performance study of novel photocatalytic reactors for decolourisation of textile dyeing wastewaters, Ind. J. Chem. Technol., 10 (2003) 638–643.

[13] R. Thiruvenkatachari, S. Vigneswaran, I.S. Moon, A review on UV/TiO_2 photocatalytic oxidation process, Korean J. Chem. Eng., 25(1) (2008) 64–72.

[14] H. Khalilian, M. Behpoura, V. Atoufa, S.N. Hosseini, Immobilization of S, N-codoped TiO_2 nanoparticles on glass beads for photocatalytic degradation of methyl orange by fixed bed photoreactor under visible and sunlight irradiation, Sol. Energy, 112 (2015) 239–245.

[15] C. Singh, R. Chaudhary, K. Gandhi, Preliminary study on optimization of pH, catalyst and oxidant dose for high COD content: solar parabolic trough collector, Iranian J. Environ. Health Sci. Eng., 10 (2013) 13.

[16] R.F.P. Nogueira, W.F. Jardim, TiO_2-Fixed-Bed reactor for water decontamination using solar light, Sol. Energy., 56(5) (1996) 471–477.

[17] T. Velegraki, D. Mantzavinos, Solar photo-Fenton treatment of winery effluents in a pilot photocatalytic reactor, Catal. Today., 240 (2015) 153–159.

[18] F. Tisa, A.A.A. Raman, W.M.A.W. Daud, Basic design of a fluidized bed reactor for wastewater treatment using Fenton oxidation, Int. J. Innovation, Manage. Technol., 5(2) (2014) 93–98.

[19] R. Dillert, S. Vollmer, M. Schober, J. Theurich, D. Bahnemann, H.J. Arntz, K. Pahlmann, J. Wienefeld, T. Schmedding, G. Sager, Photocatalytic treatment of an industrial wastewater in the double-skin sheet reactor, Chem. Eng. Tech., 22 (1999) 11.

[20] N.N. Rao, V. Chaturvedi, G. Li Pum, Novel pebble bed photocatalytic reactor for solar treatment of textile wastewater, Chem. Eng. J., 184 (2012) 90–97.

[21] A.G.G. Mata, S.V. Martínez, A.Á. Gallegos, M. Ahmadi, J.A.H. Pérez, F. Ghanbari, S.S. Martínez, Recent overview of solar photocatalysis and solar photo-Fenton processes for wastewater treatment, Int. J. Photoenergy. doi.org/10.1155/2017/8528063.

[22] APHA, AWWA and WEF, Standard Methods for the Examination of water and Wastewater. 21st ed.,. Published jointly by the American Public Health Association, American Water Works Association, and Water Environment Federation, New York. 2005.

[23] M. Ginni, S. Adishkumar, J. Rajesh Banu, I.T. Yeom, Synergistic photodegradation of pulp and paper mill wastewater by combined advanced oxidation process, Desal. Water Treat., 68 (2017) 160–169.

[24] M.F. Abid, A.A. Abdulrahman, N.H. Hamza, Hydrodynamic and kinetic study of a hybrid detoxification process with zero liquid discharge system in an industrial wastewater treatment, J. Environ. Health Sci. Eng., 12 (2014) 145.

[25] H. Sudrajat, S. Babel, A new cost-effective photocatalytic system N-ZnO@polyster fabric for degradation of recalcitrant compound in a continuous flow reactor, Mater. Res. Bull., 83 (2016) 369–378.

[26] D.A.D.A. Aljoubory, R. Senthilkumar, Phenol degradation of industrial wastewater by photocatalysis, J. Innov. Eng., 2(2) (2014) 5.

[27] I. Carra, L.S. Juanes, F.G.A. Fernández, S. Malato, J.A.S. Pérez, New approach to solar photo-Fenton operation. Raceway ponds as tertiary treatment technology, J Hazard. Mater., 279 (2014) 322–329.

[28] L. Zhoua, M. Zhoua, C. Zhanga, Y. Jiang, Z. Bia, J. Yang, Electro-Fenton degradation of p-nitrophenol using the anodized graphite felts, Chem. Eng. J., 233 (2013) 185–192.

[29] Y. Shavisi, S. Sharifnia, M. Zendehzaban, M.L. Mirghavami, S. Kakehazar, Application of solar light for degradation of ammonia in petrochemical wastewater by a floating TiO_2/LECA photocatalyst, J. Ind. Eng. Chem., 20 (2014) 2806–2813.

[30] C.A.P. Arellano, A.J. Gonzalez, S.S. Martinez, I. Salgado-Transito, C.P. Franco, Enhanced mineralization of atrazine by means of photodegradation processes using solar energy at pilot plant scale, J. Photochem. Photobiol. A: Chem., 272 (2013) 21–27.

[31] A.M.A. Pintor, V.J.P. Vilar, R.A.R. Boaventura, Decontamination of cork wastewaters by solar-photo-Fenton process using cork bleaching wastewater as H_2O_2 source, Sol. Energy, 85 (2011) 579–587.

[32] S. Lam, J. Sin, A.Z. Abdullah, A.R. Mohamed, Photocatalytic degradation of resorcinol, an endocrine disrupter, by TiO_2 and ZnO suspensions, Environ. Technol., 34(9) (2013) 1097–1106.

[33] A. Mirzaei, L. Yerushalmi, Z. Chen, F. Haghighat, J. Guo, Enhanced photocatalytic degradation of sulfamethoxazole by zinc oxide photocatalyst in the presence of fluoride ions: Optimization of parameters and toxicological evaluation, Water Res., 132 (2018) 241–251.

[34] J.B. Galvez, S.M. Rodriguez, Solar Detoxification Plataform a Solar De Almeria, Spain.

[35] E. De Torres-Socias, L.P. Rodriguez, A. Zapata, I.F. Calderero, I. Oller, S. Malato, Detailed treatment line for a specific landfill leachate treatment remediation: Brief economic assessment, Chem. Eng. J., 261(2015) 60–66.

[36] I. Michael, A. Panagi, L.A. Ioannou, Z. Frontistis, D. Fatta-Kassinos, Utilizing solar energy for the purification of olive mill wastewater using a pilot-scale photocatalytic reactor after coagulation-flocculation, Water Res., 60 (2014) 28–40.

37] G. Selvabharathi, S. Adishkumar, S. Jenefa, G. Ginni, J. Rajesh Banu, I.T. Yeom, Combined homogeneous and heterogeneous advanced oxidation process for the treatment of tannery wastewaters, J. Water Reuse Desal., (2016) 59–71.